# Measurement sensitivity dependencies on incident power and spatial resolution in slope-assisted Brillouin optical correlation-domain reflectometry

Heeyoung Lee\*, Yosuke Mizuno, Kentaro Nakamura

*Institute of Innovative Research, Tokyo Institute of Technology, 4259, Nagatsuta-cho, Midori-ku, Yokohama 226-8503, Japan*

### ABSTRACT

To enable high-speed distributed strain and temperature measurements, we have recently developed a new configuration of Brillouin optical correlation-domain reflectometry (BOCDR), called slope-assisted (SA-) BOCDR, which exploits the slope power of the Brillouin gain spectrum. Although its fundamental operations have been already clarified, a detailed study on the measurement sensitivity has not been performed yet. Here, we investigate the influences of the incident power and the spatial resolution on the measurement sensitivity of SA-BOCDR. The sensitivity is found to be improved with increasing incident power and/or lowering spatial resolution, which is verified through distributed temperature measurements.

© 2017 Elsevier B.V. All rights reserved.

## 1. Introduction

As a promising method for detecting damages of civil infrastructures, distributed fiber-optic sensing techniques based on Brillouin scattering [1] have been extensively studied for the past several decades, and numerous configurations have been developed for more sophisticated damage inspections [2–7]. Each configuration has its own advantages and disadvantages and is being extensively studied [8–20]. In particular, Brillouin optical correlation-domain reflectometry (BOCDR) [6,8] is the only technique that can simultaneously achieve intrinsically single-end accessibility and high spatial resolution. Hence, ever since it was first proposed in 2008, various schemes of BOCDR have been implemented to improve its performance, such as measurement range [13], spatial resolution [21], and sampling rate [22]. One of the newly developed configurations is slope-assisted (SA-) BOCDR [23], which uses the slope power of the Brillouin gain spectrum (BGS) to deduce the Brillouin frequency shift (BFS), leading to a high sampling rate, loss-point detectability, and beyond-nominal-resolution effect [24].

Although the basic operations of SA-BOCDR have been well characterized using both silica fibers [23,24] and polymer optical fibers

[25], no reports have been provided regarding the influences of the experimental conditions on the measurement sensitivity. Unlike in the case of standard BOCDR, the measurement sensitivity of SA-BOCDR is susceptible to the variations of incident power and spatial resolution, which determine the Brillouin signal power.

In this work, first, by analyzing the BGS shape, we investigate the measurement sensitivity dependencies on the incident power and the spatial resolution in SA-BOCDR. We show that the sensitivity is enhanced with higher incident power and/or lower spatial resolution. Then, this result is verified through distributed temperature measurements.

## 2. Principles

Distributed Brillouin sensors generally operate based on the BFS dependencies on strain and temperature [2–7]. As already mentioned, BOCDR is the only technique with intrinsic single-end accessibility and relatively high spatial resolution [6,8]. This system resolves the sensing positions using what is called a correlation peak, which is generated in a fiber under test (FUT) by sinusoidally modulating the laser output frequency. The position of the correlation peak can be continuously scanned along the FUT by sweeping the modulation frequency $f_m$; in this manner, distributed BFS measurements can be conducted. Sinusoidal frequency modulation leads to multiple correlation peaks generated along the

\* Corresponding author.
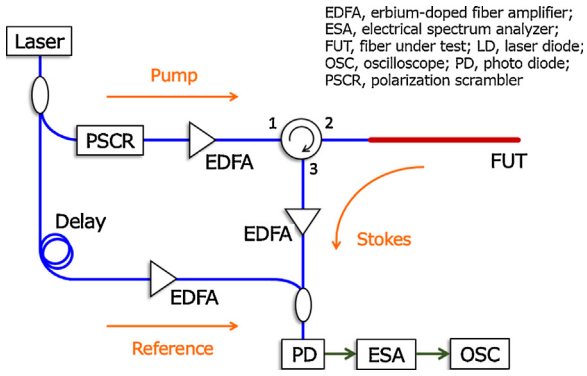    *E-mail address:* hylee@sonic.pi.titech.ac.jp (H. Lee).

**Fig. 1.** Experimental setup for SA-BOCDR.

FUT periodically, and the measurement range $d_m$ (interval of the correlation peaks) is given by the modulation frequency $f_m$ as [8]

$$d_m = \frac{c}{2nf_m}, \tag{1}$$

where $c$ is the velocity of light in a vacuum and $n$ is the core refractive index. When $f_m$ is lower than the Brillouin bandwidth $\Delta n_B$ (approximately 30 MHz in silica single-mode fibers (SMFs); dependent on incident optical power [26]), the spatial resolution $\Delta z$ is given by [8]

$$\Delta z = \frac{c \, \Delta \nu_B}{2\pi nf_m \Delta f}, \tag{2}$$

where $\Delta f$ is the modulation amplitude of the optical frequency.

In standard BOCDR, the strain (or temperature) information at one sensing position is determined from a peak frequency (i.e., BFS) after acquiring the whole BGS [6,8]. In contrast, in SA-BOCDR, the strain (or temperature) information is obtained using not the BFS itself but the spectral power change at a fixed frequency $\nu_{B0}$ (based on its one-to-one correspondence with the BFS) [23]. As a result, the BFS distribution along the FUT is obtained as a power-change distribution in SA-BOCDR. The measurement range and the nominal spatial resolution are given by the same equations as those for standard BOCDR (Eqs. (1) and (2)).

## 3. Experimental setup

In the experiment, we employed a 3.0-m-long silica SMF as an FUT. The experimental setup depicted in Fig. 1 is basically the same as that previously used [23,24]. The output from a 1.55 μm laser (3 dB bandwidth: ~1 MHz, power: 4 dBm) was divided into two light beams, pump and reference. The incident power to the FUT was changed by adjusting the output power of an erbium-doped fiber amplifier (EDFA) in the pump path. The backscattered Stokes light was amplified to ~1 dBm using another EDFA and heterodyned with the reference light, which was amplified to ~3 dBm after passing through a 1-km-long delay line (used to control the order of the correlation peak generated in the FUT). The heterodyned signal was converted to an electrical signal using a photo diode (PD). The polarization state was scrambled to suppress the polarization-dependent signal fluctuations. The video bandwidth and the resolution bandwidth of the electrical spectrum analyzer (ESA) were set to 10 kHz and 10 MHz, respectively.

The modulation frequency $f_m$ and amplitude $\Delta f$ were set to 10.858 MHz (swept from 10.825 to 10.891 MHz for distributed measurement) and 0.06–3.08 GHz, respectively, corresponding to a measurement range of ~9.5 m and a theoretical spatial resolution of 1.65–0.03 m according to Eqs. (1) and (2). For each measurement, $\nu_{B0}$ was adjusted to maximize the linear range (i.e., strain/temperature dynamic range) by differentiating the spectral
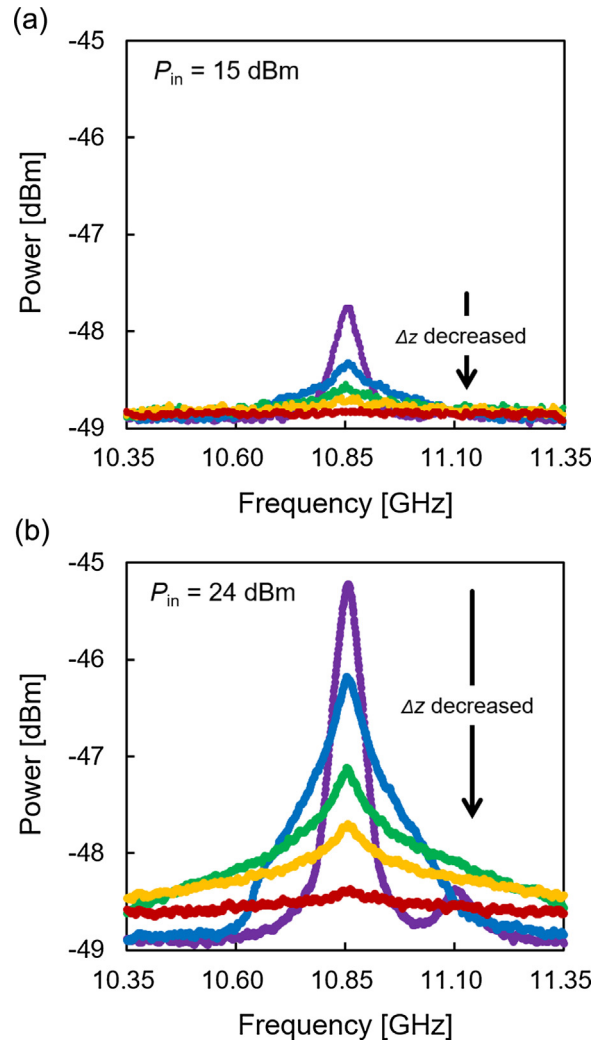


**Fig. 2.** Examples of the BGS when the spatial resolution $\Delta z$ was 1.65 (purple), 0.43 (aqua), 0.18 (green), 0.09 (yellow), and 0.03 m (red). (a) Measured at 15-dBm incident power. (b) Measured at 24-dBm incident power. (For interpretation of the references to colour in this figure legend, the reader is referred to the web version of this article.)

slope; refer to [23] for the details. The repetition rate was set to 100 Hz, and 128 times averaging was performed on the oscilloscope to obtain a sufficiently high signal-to-noise ratio. The room temperature was 21 °C.

## 4. Experimental results

First, to clarify the measurement sensitivity (defined as a spectral slope at $\nu_{B0}$) at each incident power and spatial resolution, we obtained the BGS at incident powers from 9 to 27 dBm (step: 3 dB), while the spatial resolution was simultaneously varied in the range from 0.03 to 1.65 m. Examples of the BGS measured at 15 and 24 dBm are shown in Figs. 2 (a) and 1 (b), respectively. In both cases, the BGS gradually became weaker and broader as the spatial resolution grew higher (the value itself became smaller), which leads to the reduction in its spectral slope. Here, the reduction in the peak power is natural if we simply consider that the Brillouin signal returns only from the fiber section roughly equal to the spatial resolution. The broadening of the bandwidth caused by the frequency modulation has also been reported [8]. Note that, in Fig. 1(b), when the spatial resolution was 1.65 m, an irregular peak was observed at ~11.1 GHz. This peak, which originated from the
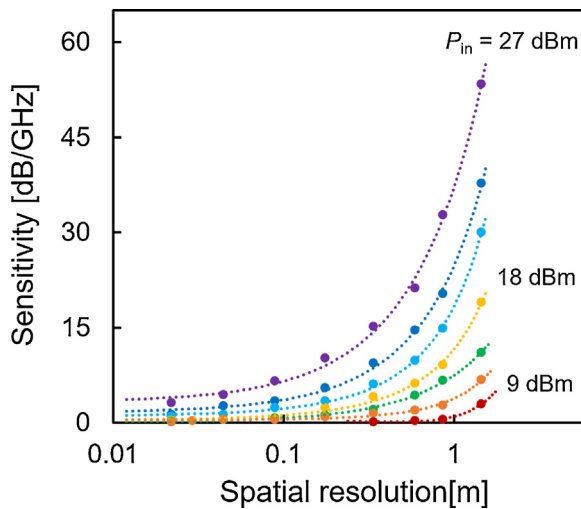
**Fig. 3.** Measurement sensitivities plotted as functions of the spatial resolution at incident powers from 9 to 27 dBm (step: 3 dB).



**Fig. 4.** Normalized power-change distributions along the FUT measured at four experimental conditions. The solid curves are measured data, and the dotted curves are calculated trends. The inset indicates the structure of the FUT.

2nd-order Brillouin peak [26], immediately disappeared by increasing modulation amplitude and did not influence the results of this measurement.

We then precisely analyzed the spectral slopes of each BGS and investigated the measurement sensitivity dependence on the spatial resolution. Here, the values of the optimal fixed frequency $v_{B0}$ (at which the slope power is measured) and the bandwidth of the linear region $w_L$ (which is evaluated by differentiating the spectral slope; refer to [23] for its detailed definition) were calculated for each BGS. For instance, when the incident power was 24 dBm and the spatial resolution was 1.65 m, $v_{B0}$ was set to 10.83 GHz and $w_L$ was approximately 50 MHz (10.78–10.83 GHz). Fig. 3 shows the measurement sensitivities plotted as functions of the spatial resolution at seven different incident powers. Regardless of the incident power, the measurement sensitivity decreased and finally converged to 0 dB/GHz as the spatial resolution grew higher (the value of the resolution itself grew smaller). At 9-dBm incident power, it was difficult to calculate the BGS slopes when the spatial resolution was lower than ∼0.3 m, because the BGS was buried by the noise. Note that, as Brillouin-scattered power does not generally increase in proportion to increasing incident power [1], we did not normalize the plots in Fig. 3. Note also that, though the temperature dynamic range seems to be dependent on incident power and spatial resolution as well, it cannot be simply evaluated by the range of the linear region because of the structural noise floor unique to correlation-domain techniques [27].

Subsequently, we performed distributed temperature measurements to verify that the results shown in Fig. 3 (indirectly acquired based on the analysis of the BGS slope) can be practically employed. The structure of the FUT is depicted in the inset of Fig. 4. While maintaining the temperature of a 0.30-m-long section (1.7 m away from the proximal FUT end) at 60 °C using a heater, the power-change distributions along the FUT were obtained under the following four experimental conditions: (incident power $P_{in}$, spatial resolution $\Delta z$) = (15 dBm, 0.09 m), (15 dBm, 0.18 m), (24 dBm, 0.09 m), and (24 dBm, 0.18 m). Fig. 4 shows the power-change distributions; the vertical axis was normalized so that the maximal value became 1 when ($P_{in}$, $\Delta z$) = (24 dBm, 0.18 m). Note that the proportions among the four data on the vertical axis were maintained. The maximal value of each data were in good agreement with the trends (shown as dotted curves in Fig. 3) calculated using Fig. 3. Note that, in the calculation, the shape of the correlation peak was assumed to be a rectangle (refer to [24]), which is not accurate. The discrepancy between the measured data and the calculated trends seems to be
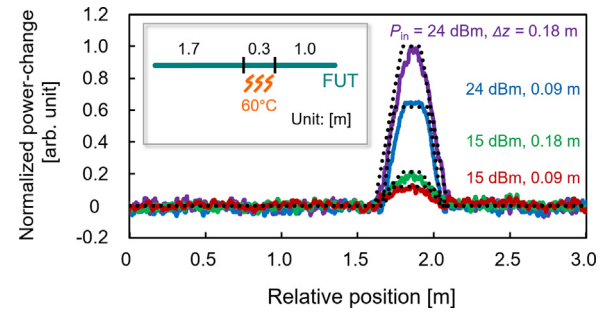
partially caused by this assumption. For each power-change distribution, we measured the standard deviation of the noise floor (signal fluctuations of the non-heated sections). Under the four experimental conditions: ($P_{in}$, $\Delta z$) = (15 dBm, 0.09 m), (15 dBm, 0.18 m), (24 dBm, 0.09 m), and (24 dBm, 0.18 m), the standard deviations (unit: °C) were calculated to be approximately 4.8, 3.3, 1.2, and 0.9 °C, respectively. The sensing error decreased with increasing measurement sensitivity (increasing incident power and/or lowering spatial resolution). Note that these values are also affected by other experimental parameters, such as the measurement speed, the number of averaging, etc. Thus, higher-power light was confirmed to be required to enhance the measurement sensitivity as well as the signal-to-noise ratio. However, injection of extremely high-power light sometimes induces a so-called optical fiber fuse phenomenon, which destroys the sensing fiber [28–30]. Consequently, the optimal incident power will be approximately 25 dBm, which should be increased or decreased considering the actual situations.

## 5. Conclusion

Based on the analysis of the BGS shape, we investigated the measurement sensitivity dependencies on the incident power and the spatial resolution in SA-BOCDR. The sensitivity decreased and then converged to 0 dB/GHz as the incident power decreased and/or the spatial resolution grew higher. Then, we verified this result through distributed temperature measurements. Thus, we believe that this work will provide a useful guideline in setting the experimental conditions of SA-BOCDR and then in achieving single-end-access high-speed distributed sensing with high spatial resolution in the future.

## References

[1] G.P. Agrawal, Nonlinear Fiber, Academic Optics Press, U.S.A., California, 2006.
[2] T. Horiguchi, M. Tateda, BOTDA-nondestructive measurement of single-mode optical fiber attenuation characteristics using Brillouin interaction: theory, J. Lightwave Technol. 7 (1989) 1170–1176.
[3] T. Kurashima, T. Horiguchi, H. Izumita, S. Furukawa, Y. Koyama, Brillouin optical-fiber time domain reflectometry, IEICE Trans. Commun. E76-B (1993) 382–390.

[4] D. Garus, K. Krebber, F. Schliep, T. Gogolla, Distributed sensing technique based on Brillouin optical-fiber frequency-domain analysis, Optics Lett. 21 (1996) 1402–1404.

[5] K. Hotate, T. Hasegawa, Measurement of Brillouin gain spectrum distribution along an optical fiber using a correlation-based technique—proposal, experiment and simulation, IEICE Trans. Electron. E83-C (2000) 405–412.

[6] Y. Mizuno, W. Zou, Z. He, K. Hotate, Proposal of Brillouin optical correlation-domain reflectometry (BOCDR), Opt. Express 16 (2008) 12148–12153.

[7] A. Minardo, R. Bernini, R. Ruiz-Lombera, J. Mirapeix, J.M. Lopez-Higuera, L. Zeni, Proposal of Brillouin optical frequency-domain reflectometry (BOFDR), Opt. Express 24 (2016) 29994–30001.

[8] Y. Mizuno, W. Zou, Z. He, K. Hotate, Operation of Brillouin optical correlation-domain reflectometry: theoretical analysis and experimental validation, J. Lightw. Technol. 28 (2010) 3300–3306.

[9] X. Bao, L. Chen, Recent progress in distributed fiber optic sensors, Sensors 12 (2012) 8601–8639.

[10] N. Hayashi, K. Minakawa, Y. Mizuno, K. Nakamura, Brillouin frequency shift hopping in polymer optical fiber, Appl. Phys. Lett. 105 (2014) 091113.

[11] Y. Peled, A. Motil, M. Tur, Fast Brillouin optical time domain analysis for dynamic sensing, Opt. Express 20 (2012) 8584–8591.

[12] W. Zou, Z. He, K. Hotate, Range elongation of distributed discrimination of strain and temperature in Brillouin optical correlation-domain analysis based on dual frequency modulations, IEEE Sens. J. 14 (2014) 244–248.

[13] Y. Mizuno, Z. He, K. Hotate, Measurement range enlargement in Brillouin optical correlation-domain reflectometry based on double-modulation scheme, Opt. Express 18 (2010) 5926–5933.

[14] Y. Dong, H. Zhang, L. Chen, X. Bao, 2 cm spatial-resolution and 2 km range Brillouin optical fiber sensor using a transient differential pulse pair, Appl. Opt. 51 (2012) 1229–1235.

[15] J. Urricelqui, A. Zornoza, M. Sagues, A. Loayssa, Dynamic BOTDA measurements based on Brillouin phase-shift and RF demodulation, Opt. Express 20 (2012) 26942–26949.

[16] Y. Dong, P. Xu, H. Zhang, Z. Lu, L. Chen, X. Bao, Characterization of evolution of mode coupling in a graded-index polymer optical fiber by using Brillouin optical time-domain analysis, Opt. Express 22 (2014) 26510–26516.

[17] D. Zhou, Y. Dong, B. Wang, H. Li, Slope-assisted BOTDA based on vector SBS and frequency-agile technique for wide-strain-range dynamic measurements, Opt. Express 25 (2017) 1889–1902.

[18] M.A. Soto, L. Thevenaz, Modeling and evaluating the performance of Brillouin distributed optical fiber sensors, Opt. Express 21 (2013) 31347–31366.

[19] D. Ba, D. Zhou, B. Wang, Z. Lu, Z. Fan, Y. Dong, H. Li, Dynamic distributed Brillouin optical fiber sensing based on dual-modulation by combining single frequency modulation and frequency-agility modulation, IEEE Photon. J. 9 (2017) 7102908.

[20] A. Motil, O. Danon, Y. Peled, M. Tur, Pump-power-independent double slope-assisted distributed and fast Brillouin fiber-optic sensor, IEEE Photon. Technol. Lett. 26 (2014) 797–800.

[21] S. Manatham, M. Kishi, Z. He, K. Hotate, 1-cm spatial resolution with large dynamic range in strain distributed sensing by Brillouin optical correlation domain reflectometry based on intensity modulation, Proc. SPIE 8351 (2012) 835136.

[22] Y. Mizuno, N. Hayashi, H. Fukuda, K.Y. Song, K. Nakamura, Ultrahigh-speed distributed Brillouin reflectometry, Light 5 (2016) e16184.

[23] H. Lee, N. Hayashi, Y. Mizuno, K. Nakamura, Slope-assisted Brillouin optical correlation-domain reflectometry: proof of concept, IEEE Photon. J. 8 (2016) 6802807.

[24] H. Lee, N. Hayashi, Y. Mizuno, K. Nakamura, Operation of slope-assisted Brillouin optical correlation-domain reflectometry: comparison of system output with actual frequency shift distribution, Opt. Express 24 (2016) 29190–29197.

[25] H. Lee, N. Hayashi, Y. Mizuno, K. Nakamura, Slope-assisted Brillouin optical correlation-domain reflectometry using polymer optical fibers with high propagation loss, J. Lightwave Technol. 35 (2016) 2306–2310.

[26] A. Yeniay, J.-M. Delavaux, J. Toulouse, Spontaneous and stimulated Brillouin scattering gain spectra in optical fibers, J. Lightwave Technol. 20 (2002) 1425–1432.

[27] K.Y. Song, Z. He, K. Hotate, Optimization of Brillouin optical correlation-domain analysis system based on intensity modulation scheme, Opt. Experss 14 (2006) 4256–4263.

[28] S. Todoroki, In-situ observation of fiber-fuse propagation, Jpn. J. Appl. Phys. 44 (2005) 4022–4024.

[29] Y. Mizuno, N. Hayashi, H. Tanaka, K. Nakamura, S. Todoroki, Observation of polymer optical fiber fuse, Appl. Phys. Lett. 104 (2014) 043302.

[30] Y. Mizuno, N. Hayashi, H. Tanaka, K. Nakamura, Spiral propagation of polymer optical fiber fuse accompanied by spontaneous burst and its real-time monitoring using Brillouin scattering, IEEE Photon. J. 6 (2014) 6600307.

## Biographies



**Heeyoung Lee** received the B.E. degree in mechanical engineering from Kyungpook National University, Korea, in 2014, and the M.E. degree in information processing from Tokyo Institute of Technology, Japan, in 2017. She has been continuing to study fiber-optic sensors for her Dr.Eng. degree at Tokyo Institute of Technology. She is currently a Research Fellow (DC1) of the Japanese Society for the Promotion of Science (JSPS).



**Yosuke Mizuno** received the B.E., M.E., and Dr.Eng. degrees in electronic engineering from the University of Tokyo, Japan, in 2005, 2007, and 2010, respectively. Since 2012, he has been an Assistant Professor at the Precision and Intelligence Laboratory (presently, Institute of Innovative Research), Tokyo Institute of Technology, where he is active in fiber-optic sensing, polymer optics, and ultrasonics.



**Kentaro Nakamura** received the B.E., M.E., and Dr.Eng. degrees from Tokyo Institute of Technology, Japan, in 1987, 1989, and 1992, respectively. Since 2010, he has been a Professor at the Precision and Intelligence Laboratory (presently, Institute of Innovative Research), Tokyo Institute of Technology. His research field is the applications of ultrasonic waves, measurement of vibration and sound using optical methods, and fiber-optic sensing.